


# The RNA m6A-Binding Protein YTHDC1 Is Downregulated and Associated With M2 Macrophage Infiltration in Muscle-Invasive Bladder Cancer

Lamei Zhao<sup>1,2\*</sup>, Dongyan Han<sup>2\*</sup>, Jianghua Zhu<sup>3\*</sup>, Dexi Bi<sup>2</sup>, Tingting Ding<sup>2</sup>, Xingchen Zhu<sup>2</sup>, Dengfeng Huang<sup>2</sup>, Youhua Zhang<sup>2</sup>, Ling Lu<sup>2</sup>, Weijun Wu<sup>2</sup>, Yaohui Gao<sup>2</sup>, Hu Liu<sup>2</sup>, Qiongyi Huang<sup>2</sup>, Qing Wei<sup>1,2</sup>  and Xudong Yao<sup>4</sup>

<sup>1</sup>Shanghai Clinical College, Anhui Medical University, Hefei, China. <sup>2</sup>Department of Pathology, Shanghai Tenth People's Hospital, Tongji University School of Medicine, Shanghai, China.

<sup>3</sup>Medical Equipment of Shanghai Tenth People's Hospital, Tongji University School of Medicine, Shanghai, China. <sup>4</sup>Department of Urology, Shanghai Tenth People's Hospital, Tongji University School of Medicine, Shanghai, China

Clinical Medicine Insights: Oncology

Volume 17: 1–8

© The Author(s) 2023

Article reuse guidelines:

sagepub.com/journals-permissions

DOI: 10.1177/11795549231203150



## ABSTRACT

**BACKGROUND:** Dysregulation of RNA N6-methyladenosine (m6A) modification is indispensable in tumorigenesis. However, in muscle-invasive bladder cancer (MIBC), the key regulators and mechanisms involved in this process remain largely unknown. This study aimed to screen the key m6A regulators and explore its possible role in MIBC.

**METHODS:** Aberrantly expressed m6A regulator genes were screened in The Cancer Genome Atlas (TCGA) MIBC cohort (n = 408) and validated using fresh-frozen and formalin-fixed paraffin-embedded (FFPE) specimens collected during this study. Clinicopathological relevance and association with tumor immune infiltration was further assessed.

**RESULTS:** We identified that the expression of YT521-B homology-domain-containing protein 1 (YTHDC1), an m6A RNA-binding protein, was downregulated in tumor tissues compared with adjacent noncancerous tissues in the TCGA MIBC cohort and our clinical samples. Low *YTHDC1* expression correlated with short patient survival, advanced pathologic stage, lymph node metastasis, basal-squamous molecular subtype, non-papillary histological type, and certain genetic mutations important to MIBC. Remarkably, *YTHDC1* expression exhibited negative association with tumor-infiltrating M2 macrophage abundance in MIBC.

**CONCLUSION:** Among m6A regulators, we identified that YTHDC1 was downregulated in MIBC and might play an important role in the pathological process in MIBC, especially tumor microenvironment regulation.

**KEYWORDS:** YTHDC1, muscle-invasive bladder cancer, M2 macrophage, tumor microenvironment

**RECEIVED:** March 28, 2023. **ACCEPTED:** September 8, 2023.

**TYPE:** Original Research Article

**FUNDING:** The author(s) disclosed receipt of the following financial support for the research, authorship, and/or publication of this article: This study was supported by the National Natural Science Foundation of China (82072634 to Q.W.).

**DECLARATION OF CONFLICTING INTERESTS:** The author(s) declared no potential conflicts of interest with respect to the research, authorship, and/or publication of this article.

**CORRESPONDING AUTHORS:** Qing Wei, Department of Pathology, Shanghai Tenth People's Hospital, Tongji University School of Medicine, 301 Yanchang Road, Shanghai 200272, China. Email: weiqing1971@126.com

Xudong Yao, Department of Urology, Shanghai Tenth People's Hospital, Tongji University School of Medicine, 301 Yanchang Road, Shanghai 200072, China. Email: yaoxudong67@sina.com

## Introduction

Bladder cancer is the tenth most commonly diagnosed cancer worldwide.<sup>1</sup> More than 90% of bladder cancers originate from the urothelium epithelium of bladder. Tumors invading the muscle or beyond are called muscle-invasive bladder cancer (MIBC), while those not are non-muscle-invasive bladder cancer (NMIBC). At initial diagnosis, approximately 30% are already MIBC. In addition, at least 21% high-risk NMIBC may progress to MIBC.<sup>2</sup> Patients with MIBC usually have poor prognosis. Even for those without metastasis, the 5-year overall survival (OS) rate is only 36% to 48%.<sup>2</sup> Novel biomarkers contributing to improving MIBC diagnosis and therapy are still in need.

N6-methyladenine (m6A) modification is the most abundant form of posttranscriptional RNA modification in

eukaryotes, which influences multiple processes of RNA metabolism.<sup>3</sup> The RNA m6A modification is dynamically and reversibly modulated by 3 types of regulators, the m6A methyltransferases that install the modification (“writers”), m6A demethylases that remove the modification (“erasers”), and m6A RNA-binding protein (“readers”) sites that recognize m6A sites and mediate various downstream biological functions.<sup>4</sup> In recent years, increasing evidence shows that m6A regulators also play key roles in tumorigenesis and progression. For example, METTL3, an m6A methyltransferase, is reported to promote hepatocellular carcinoma (HCC) tumorigenesis and lung metastasis through reducing SOCS2 expression via an m6A- and YTHDF2-dependent mechanism.<sup>5</sup> ALKBH5, an m6A demethylase, could enhance FOXM1 expression by reducing m6A abundance on target mRNA transcripts and further enhanced self-renewal and proliferation of glioblastoma stem

\*Lamei Zhao, Dongyan Han, and Jianghua Zhu contributed equally to this work.



cells to promote tumorigenesis.<sup>6</sup> Notably, the YT521-B homology-domain-containing protein 1 (YTHDC1), a versatile m6A reader<sup>7</sup> regulating nuclear RNA splicing, alternative polyadenylation, nuclear export, and decay,<sup>8-13</sup> also plays different roles in the development of many human diseases, such as the acute myeloid leukemia (AML),<sup>14</sup> non-small cell lung cancer,<sup>15</sup> renal cell carcinoma,<sup>16</sup> glioblastoma,<sup>17</sup> pancreatic ductal adenocarcinoma,<sup>18</sup> and breast cancer.<sup>19</sup> However, the involvement of m6A modification dysregulation in MIBC and relevant mechanisms remain largely unelucidated.

In this study, we aimed to explore the role of m6A regulators in MIBC pathogenesis. Aberrantly expressed m6A-related regulators were screened and clinicopathological relevance was assessed, which revealed that YTHDC1 was downregulated in tumor and negatively associated with M2 macrophage infiltration. This study helps to understand the dysregulation of m6A modification in MIBC.

## Materials and Methods

### *Ethics*

This study was approved by the Ethics Committee of Shanghai Tenth People's Hospital (SHYS-IEC-5.0/22K243/P01) and the written informed consent was waived due to the retrospective nature of the study and the reanalysis of the samples already archived in the BioBank of Shanghai Tenth People's Hospital.

### *The Cancer Genome Atlas dataset*

The RNA-Seq data of 408 tumor tissues and 19 adjacent normal tissues of patients with MIBC along with the corresponding clinicopathological information in The Cancer Genome Atlas (TCGA) were obtained from the UCSC Xena platform (<https://xena.ucsc.edu/public>).<sup>20</sup> The expression data of 32 genes that have been identified as m6A regulators (Supplemental Table S1) were extracted for analysis. The log<sub>2</sub>-transformed upper-quartile-normalized fragments per kilobase million were used.

### *Patients and tissue samples*

Tumor and matched adjacent normal tissue samples were collected from patients with MIBC receiving radical cystectomy at the Shanghai Tenth People's Hospital from March 2010 to June 2019. Fresh-frozen tissue samples were collected from 23 patients. For each of the samples, a portion of freshly resected tissue was snap-frozen immediately in liquid nitrogen and stored at -80°C. Clinical formalin-fixed paraffin-embedded (FFPE) tissue samples were collected from an independent cohort of 59 patients with MIBC.

### *RNA extraction and quantitative reverse transcription PCR*

Total RNA was extracted from the fresh-frozen tissue samples with the TRIzol reagent (Invitrogen, Carlsbad, CA) according

to manufacturer's instruction and reversely transcribed into cDNA with the PrimeScript RT Master Mix (Takara, Kyoto, Japan) on a Mastercycler (Eppendorf, Germany). For each reverse transcription reaction, 1 µg RNA was used and the conditions were 37°C for 15 minutes, 95°C for 5 seconds, and 4°C for 10 minutes. Quantitative polymerase chain reaction (PCR) was then performed with 2 µL of the above cDNA products and the TB Green Premix Ex Taq II (Takara, Kyoto, Japan) kit on an ABI Prism 7500 Sequence Detection System (Applied Biosystems, Foster City, CA). The conditions were 50°C for 2 minutes, 95°C for 30 seconds, 40 cycles of 95°C for 5 seconds, 50°C for 34 seconds, and 70°C for 30 seconds, and finally 4°C for 10 minutes. The primer sequences were 5'-TCAGGA GTTCGCCGAGATGTGT-3' (forward) and 5'-AGGATG GTGTGGAGGTTGTTCC-3' (reverse) for *YTHDC1*; and 5'-ACAGTCAGCCGCATCTTCTT-3' (forward) and 5'-GACAAGCTTCCCGTTCTCAG-3' (reverse) for *GAPDH*. Experiments were independently performed in triplicate. A mean  $-\Delta\text{Ct}$  value was calculated for each sample.

### *Tissue microarray construction*

Tissue microarrays (TMAs) were constructed as previously described.<sup>21</sup> Briefly, hematoxylin and eosin (HE)-stained section from each FFPE block was reviewed by 2 pathologists independently to confirm the histopathological diagnosis. Cylindrical cores (diameter=2 mm) extracted from the tissue samples were inserted into a recipient paraffin block in a grid pattern (6×10 matrix) with a tissue microarrayer (UNITMA Quick-Ray, UT-06).<sup>22</sup>

### *Immunohistochemistry and scoring*

Sections (3-5 µm) were cut from the TMAs and placed on polylysine-coated slides. Subsequent deparaffinization and staining with the YTHDC1 antibody (1:100; ab122340, Abcam, USA) was carried out by Wuhan Servicebio Technology Co., Ltd. The immunohistochemistry (IHC) results were quantified by 2 pathologists independently from 2 aspects: staining intensity score (0 for negative, 1 for weak, 2 for moderate, and 3 for strong staining) and percentage of stained cells (0 for 0%, 1 for 1%-10%, 2 for 11%-25%, 3 for 26%-50%, 4 for 51%-75%, and 5 for 76%-100%).<sup>21</sup> For each sample, an IHC score was calculated as the average of the product of 2 statistical scores.

### *Tumor-infiltrating immune cell abundance analysis from RNA-seq data*

The abundance of 43 tumor-infiltrating immune cells based on the RNA-seq data of 408 patients with MIBC from the TCGA cohort was estimated by 2 different algorithms CIBERSORT and XCELL on the TIMER2.0 platform (<http://timer.comp-genomics.org/>).<sup>23</sup>

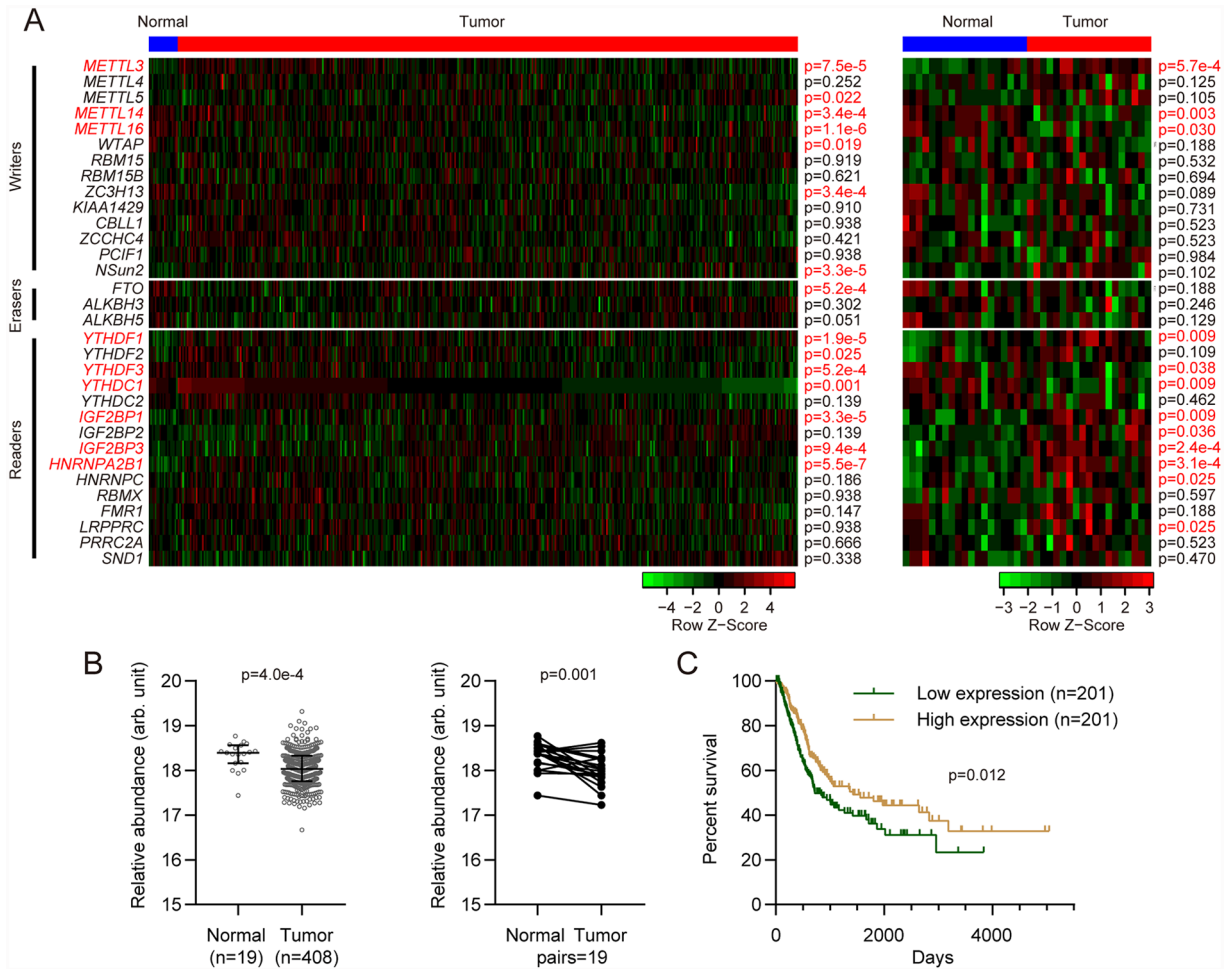


**Figure 1.** YTHDC1 is a downregulated m6A modification regulator gene in muscle-invasive bladder cancer and negatively associated with overall survival in The Cancer Genome Atlas cohort. (A) Screen for aberrantly expressed m6A regulator genes. The heatmap on the left indicates comparison between all available normal (n=19) and tumor (n=408) tissues (Mann-Whitney test), while that on the right indicates comparison between paired normal and tumor tissues of 19 patients (Wilcoxon signed-rank test). Adjusted *P* values are given (Benjamini-Hochberg method). Those  $<.05$  are marked in red as well as the corresponding gene names. (B) Comparison of relative YTHDC1 expression between all available tumor and normal tissues (left; Mann-Whitney test) and between paired normal and tumor tissues (right; Wilcoxon signed-rank test). Medians and interquartile ranges are shown. (C) Overall survival comparison between patients with high or low YTHDC1 expression levels that were separated by median (log-rank test).

### Heatmap

The heatmaps were generated by the ggplot2 or Complex Heatmap package in R as applicable.

### Statistical analysis

Statistics was performed by GraphPad Prism 9 (GraphPad Software, San Diego, CA, USA). Quantitative data were compared by Wilcoxon signed-rank test and Mann-Whitney test as applicable. For the screen of differentially expressed genes, *P* values were adjusted by the Benjamini-Hochberg method. For comparison among 3 or more groups, Kruskal-Wallis test followed by Dunn's multiple comparison was used. Categorical data were compared by chi-square test or Fisher exact test. The Kaplan-Meier curve and log-rank test were used for survival analysis. Spearman correlation test was used for correlation

analysis. A 2-tailed  $P<.05$  was considered statistically significant.

### Results

#### *YTHDC1 is a downregulated m6A modification regulator gene in MIBC in the TCGA cohort*

To explore the role of m6A regulators in MIBC, we first analyzed the expression profile of 32 m6A modification regulator genes (Supplemental Table S1) in the RNA-seq data of the TCGA MIBC cohort. Compared with normal tissues (n=19), 15 genes were found to be differentially expressed in tumor tissues (n=408) (Figure 1A). Among them, the expression of 9 genes, including 3 m6A RNA methyltransferase genes (*METTL3*, *METTL14*, and *METTL16*) and 6 m6A RNA-binding protein genes (*YTHDF1*, *YTHDF3*, *YTHDC1*, *IGF2BP1*, *IGF2BP3*, and *HNRNPA2B1*), also showed



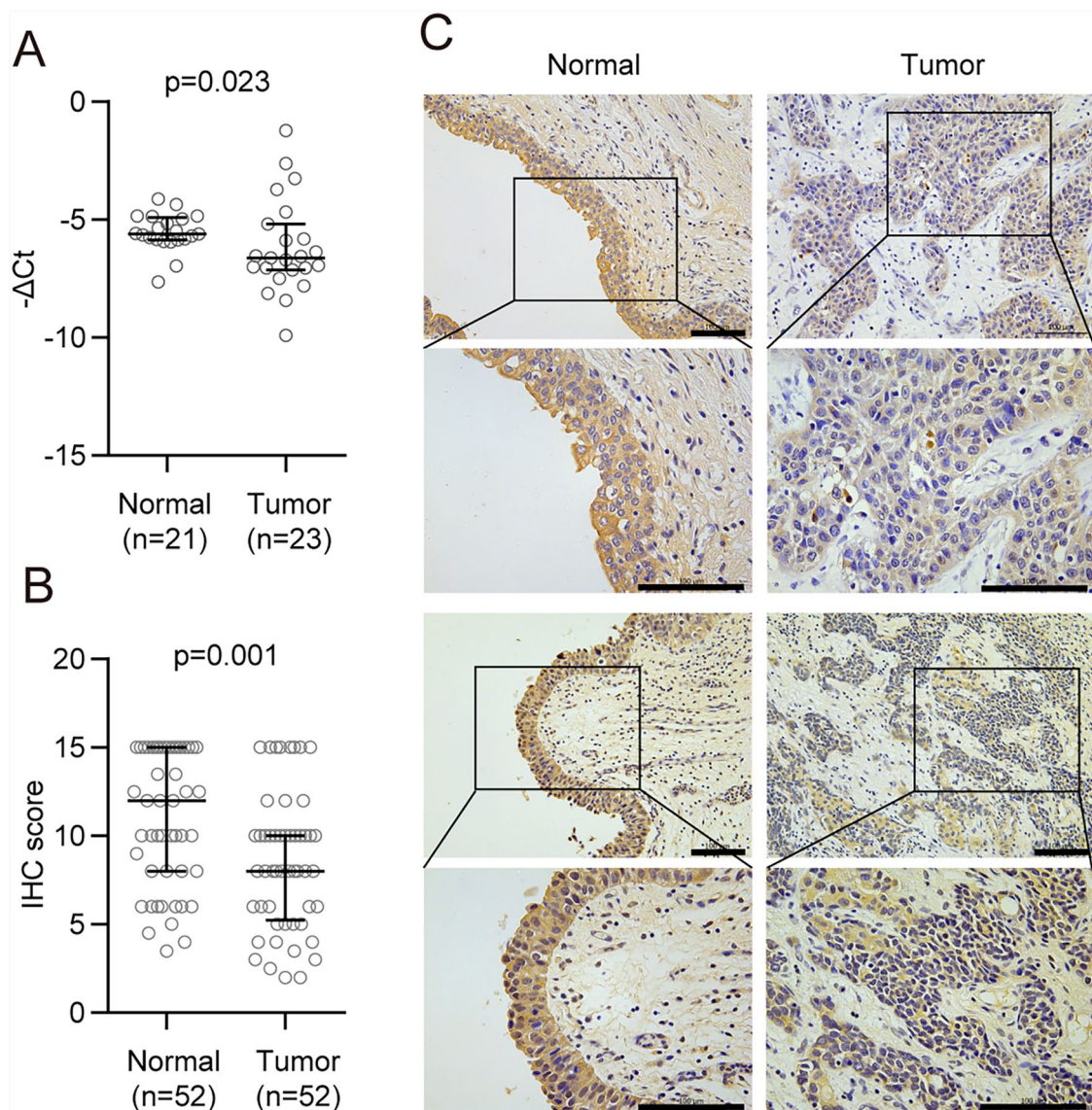


**Figure 2.** Validation in clinical samples confirmed YTHDC1 downregulation in MIBC. (A) Comparison of the relative YTHDC1 expression in 23 fresh-frozen tumor and 21 adjacent normal tissues from 23 patients with MIBC (Mann-Whitney test). (B) IHC staining scores of YTHDC1 in 52 FFPE tumor tissues and 52 adjacent normal tissues from 59 patients with MIBC (Mann-Whitney test). (C) The representative images of the YTHDC1 IHC staining in tumor and adjacent normal tissues. Scale bar, 100  $\mu$ m. Medians and interquartile ranges are shown for (A) and (B). IHC indicates immunohistochemistry; MIBC, muscle-invasive bladder cancer.

significant difference in paired comparison between tumor and matched normal tissues available in 19 cases (Figure 1A). Further survival analysis revealed that the expression of *YTHDC1* is negatively associated with OS, consistent with its downregulation in MIBC (Supplemental Figure S1 and Figure 1B). Thus, *YTHDC1* was selected for analysis in this study.

#### *Independent validation confirmed YTHDC1 is downregulated at both mRNA and protein levels in MIBC*

We next detected the mRNA and protein levels of *YTHDC1* in clinical samples from patients with MIBC to validate whether it is downregulated in MIBC. The expression of

*YTHDC1* quantified by qPCR in fresh-frozen tumor tissues (n=23) was found decreased compared with fresh-frozen normal tissues (n=21) (Figure 2A). Consistently, in an independent cohort of FFPE specimens from 59 patients with MIBC, IHC staining of *YTHDC1* indicated that the tumor tissues had lower IHC scores than normal tissues (Figure 2B and C). Those results confirmed that *YTHDC1* is downregulated in MIBC.

#### *Associations between YTHDC1 expression and clinicopathological characteristics*

We further explored the clinicopathological significance of *YTHDC1* in MIBC based on analysis of the TCGA database.

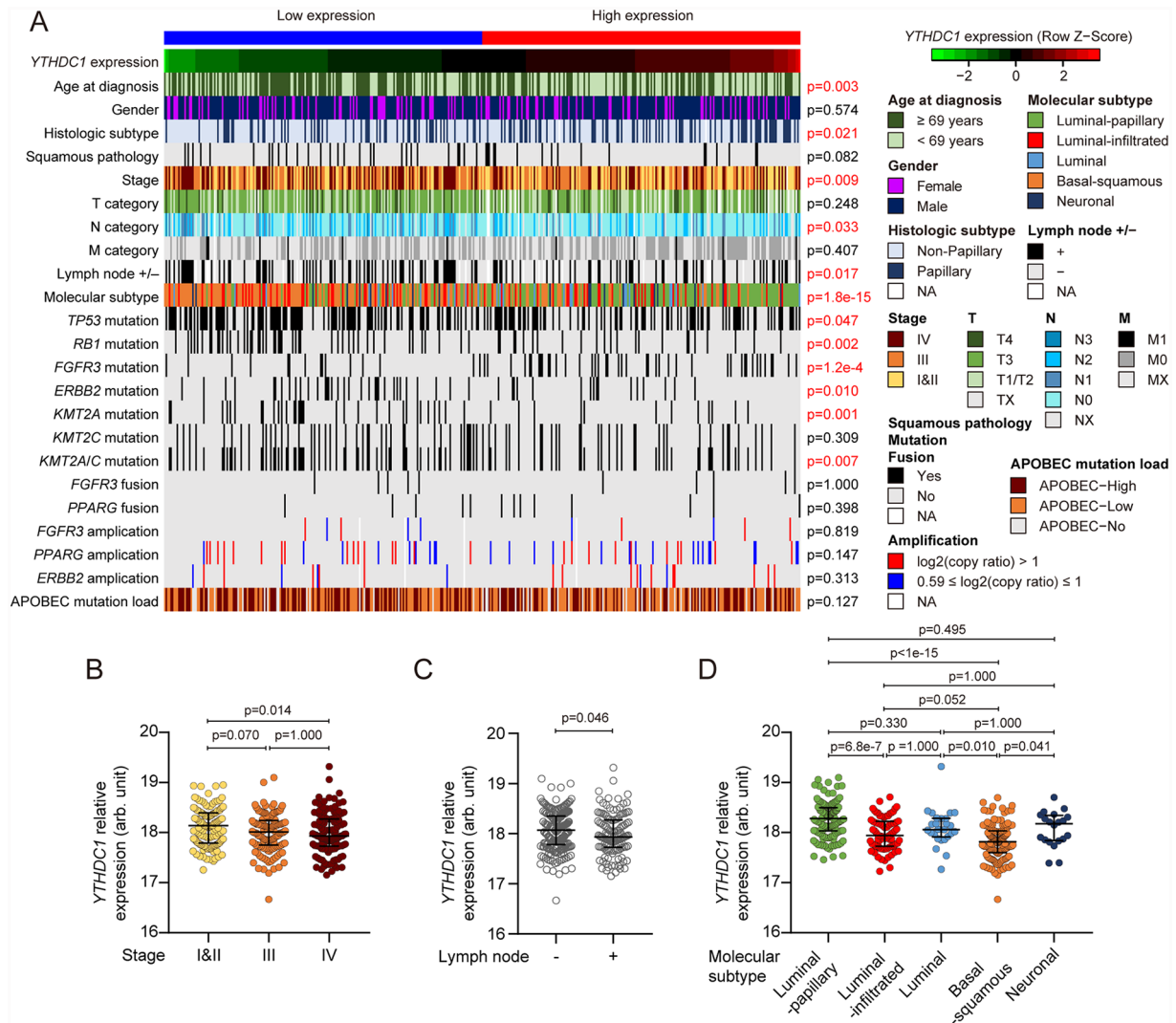


**Figure 3.** Association between YTHDC1 expression and clinical and pathological characteristics in muscle-invasive bladder cancer based on The Cancer Genome Atlas cohort. (A) A heatmap showing the YTHDC1 expression and analyzed clinical and pathological characteristics of 408 patients. P values are shown by the right of the heatmap and those  $< 0.05$  are marked in red (Chi-square test or Fisher exact test). (B) YTHDC1 expression compared by tumor stages (Kruskal-Wallis test followed by Dunn's multiple comparisons test). (C) YTHDC1 expression compared by lymph node status (Mann-Whitney test). (D) YTHDC1 expression compared by molecular subtypes (Kruskal-Wallis test followed by Dunn's multiple comparisons test). For (B-D), medians and interquartile ranges are shown.

We observed that *YTHDC1* expression exhibited associations with several key clinicopathological characteristics, including tumor stage, lymph node status, histological subtype, molecular subtype, and certain genetic mutations that are important to MIBC (Figure 3A). Low *YTHDC1* expression correlated with non-papillary histology, high tumor stages (Figure 3B), and lymph node-positive status (Figure 3C). *YTHDC1* had different expression levels across molecular subtypes with low expression mostly seen in the basal/squamous subtype (Figure 3D). But the association with disease-free survival (Supplemental Figure S2) or distant metastasis (Supplemental Figure S3) was not observed. In addition, *YTHDC1* expression shows association with *TP53*, *RB1*, *FGFR3*, *ERBB2*, *KMT2A*, or combined *KMT2A* and *KMT2C* mutation, but not with *FGFR3* or

*PPARG* fusion, *FGFR3*, *PPARG*, or *ERBB2* amplification, or APOBEC mutation load (Figure 3A).

#### Low YTHDC1 expression correlates to M2 macrophage infiltration in MIBC

We then sought to explore whether *YTHDC1* was associated with regulation of tumor microenvironment (TME), as low *YTHDC1* expression was enriched in the basal/squamous subtype that involves extensive immune infiltration and *KMT2A/C* mutations have also been reported as a biomarker for immunotherapy.<sup>24</sup> We thus conducted tumor-infiltrating immune cell abundance analysis covering 43 immune cell types from the RNA-seq data and uncovered that M2 macrophage infiltration

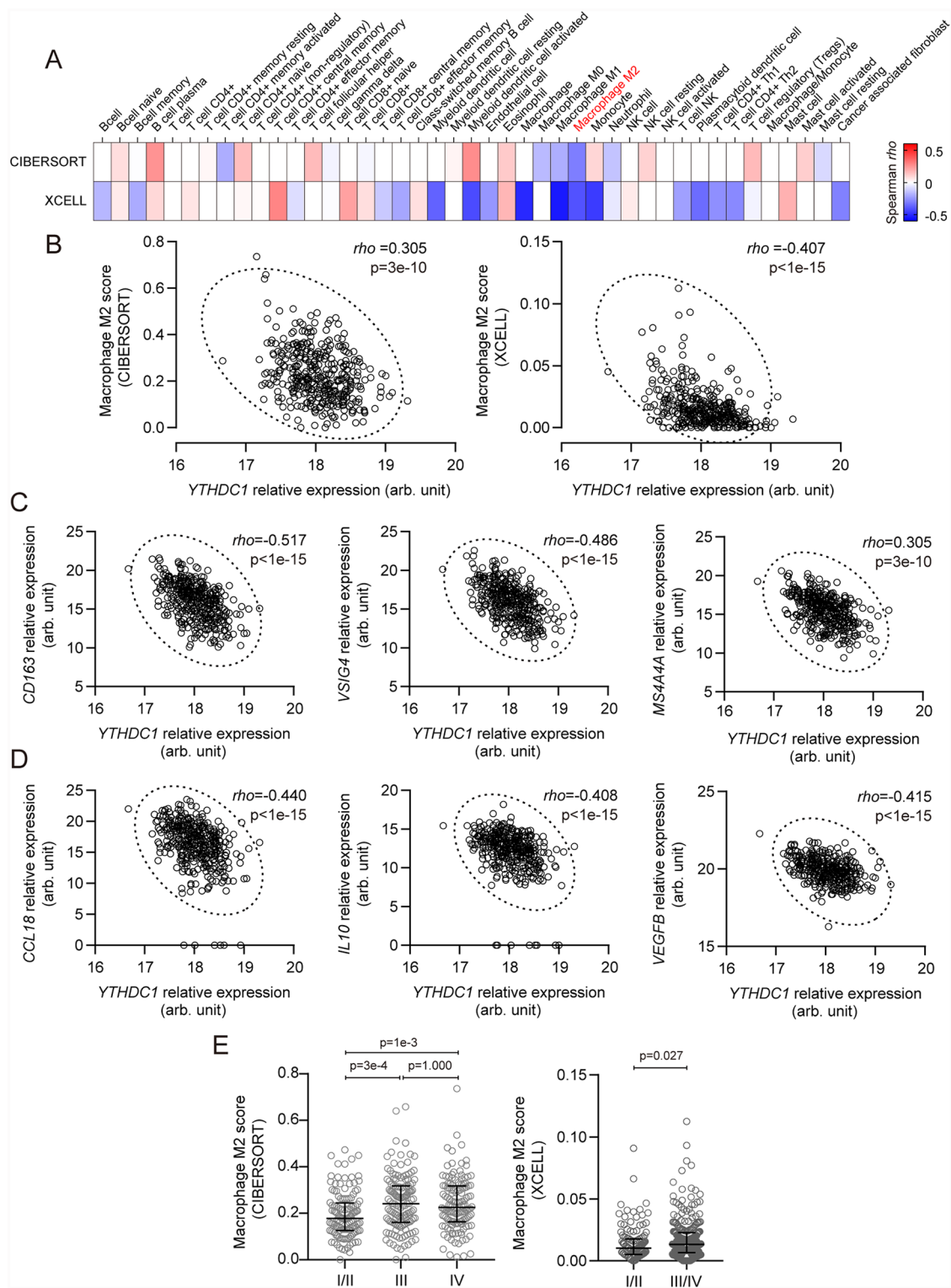


**Figure 4.** Negative correlation between *YTHDC1* expression and the infiltrating levels of M2 macrophage. (A) Correlation analysis between *YTHDC1* expression and the infiltrating level of 43 immune cell types calculated with CIBERSORT and XCELL algorithms (Spearman correlation test). (B) *YTHDC1* expression was consistently and significantly negatively correlated with the infiltrating levels of M2 macrophage as indicated by 2 algorithms. (C) *YTHDC1* expression was negatively correlated with M2 macrophage marker genes (Spearman correlation test). (D) *YTHDC1* expression was negatively correlated with M2 macrophage-associated cytokines (Spearman correlation test). (E) The infiltrating levels of M2 macrophage based on the 2 algorithms were consistently and significantly correlated with high pathologic tumor stages (left; Kruskal-Wallis test followed by Dunn's multiple comparisons test, right; Mann-Whitney test).

was negatively correlated with *YTHDC1* expression in MIBC, which were consistently supported by 2 different algorithms CIBERSORT and XCELL (Figure 4A and B). Indeed,

*YTHDC1* expression showed negative association with the expression of M2 macrophage marker genes *CD163*, *VSIG4*, and *MS444A*<sup>25</sup> as well as its cytokine genes *IL10* and *CCL18*



(Figure 4C), with *rho* values higher than those of the markers of other types of immune cells (Supplemental Table S2). In addition, high M2 macrophage infiltration also correlated with high tumor stages in MIBC (Figure 4D).

## Discussion

This study screened for m6A regulators that may be involved in MIBC and identified that YTHDC1 is downregulated in tumors. It is associated with multiple important clinicopathological features and likely plays a role in TME modulation.

The m6A RNA-binding proteins interpret m6A modification by recognizing m6A sites and mediating various downstream biological functions. YTHDC1 is an important m6A RNA-binding protein that has been reported to involve in different types of cancers via diverse mechanisms. We found that YTHDC1 was downregulated in MIBC compared with adjacent normal tissues. Further comprehensive analysis showed that *YTHDC1* expression had a significant association with molecular subtypes. While MIBC has been classified into 5 molecular subtypes with different genetic mutational signatures, clinical characteristics, prognostic features and potential therapeutic strategies, low *YTHDC1* expression mainly enriched in basal/squamous subtype, suggesting that YTHDC1 may be a potential marker of this subtype. Meanwhile, as the basal/squamous subtype is closely related to tumor immune infiltration and informs potential benefit of immunotherapy, we speculated whether YTHDC1 could be a TME modulator. Previous studies have reported that in non-small-cell lung cancer, YTHDC1 regulates m6A-mediated circIGF2BP3 back-splicing, which contributes to CD8<sup>+</sup> T-cell infiltration.<sup>15,26</sup> Here, we found that *YTHDC1* level negatively correlated with M2 macrophage infiltration in MIBC. In most cancers, the presence of M2 macrophages tends to be a negative prognostic indicator, promoting tumor progression and suppressing anti-tumor immune response.<sup>27,28</sup> It has been reported that M2 macrophages were the highest proportion of tumor-infiltrating immune cells in bladder cancer, and high M2 macrophage infiltration also correlated with unfavorable prognosis, high histologic grade, high tumor stage, and “basal” subtype,<sup>29</sup> in agreement with the *YTHDC1*-related clinicopathological features observed here. Most macrophages in TME are circulating monocytes recruited by chemotaxis signaling and then polarized into M1 macrophages or M2 macrophages under certain conditions.<sup>30</sup> Consistently, the *YTHDC1* expression was also negatively correlated with the expression of chemokine (*CCL2*, *CCL5*, *C5AR1*, and *CSF-1*) and polarization-related genes (*CEBPB*) (Supplemental Table S3). Therefore, it is likely that the m6A RNA metabolic process involving YTHDC1 could regulate chemokine and polarized cytokine levels, thereby modulating the infiltration of immunosuppressed M2 macrophages. However, further in-depth investigations are needed to clarify the underlying molecular mechanism. Based on the

findings of this study, YTHDC1 may have a potential to serve as a diagnostic and prognostic biomarker, particularly to indicate molecular features and M2 macrophage infiltration, as well as a target to facilitate immunotherapy in MIBC.

This study has limitations. The sample size of our cohort is still small. Studies with large sample size should be conducted to further validate the results generated based on the TCGA cohort. In-depth experimental investigations are also needed to decipher the molecular mechanisms underlying MIBC pathogenesis driven by YTHDC1.

## Conclusion

Among m6A regulators, we identified that YTHDC1 was downregulated in MIBC and might play an important role in the pathological process in MIBC, especially TME regulation.

## Acknowledgements

The results shown here are in part based on data generated by the TCGA Research Network: <https://www.cancer.gov/tcga>.

## Author Contributions

XY, QW, and DB designed and supervised this project. LZ, DH, JZ, and DB performed bioinformatic analyses. LZ, XZ, DH, YZ, LL, WW, YG, HL, and QH construed tissue microarrays, performed immunohistochemical staining, and analyzed the results. TD, YZ, LL, WW, and YG provided advice and supervision of the analytic process. LZ, DH, and JZ wrote original draft preparation of the article. LZ, XY, QW, and DB amended the writing of the article. All authors have read and agreed to the published version of the manuscript.

## Research Ethics and Patient Consent

This study was approved by the Ethics Committee of Shanghai Tenth People's Hospital (SHYS-IEC-5.0/22K243/P01) and the written informed consent was waived due to the retrospective nature of the study and the reanalysis of the samples already archived in the BioBank of Shanghai Tenth People's Hospital.

## ORCID iD

Qing Wei  <https://orcid.org/0000-0002-9007-5473>

## SUPPLEMENTAL MATERIAL

Supplemental material for this article is available online.

## REFERENCES

1. Sung H, Ferlay J, Siegel RL, et al. Global cancer statistics 2020: GLOBOCAN estimates of incidence and mortality worldwide for 36 cancers in 185 countries. *CA Cancer J Clin.* 2021;71:209-249.
2. Lenis AT, Lec PM, Chamie K, Mshs MD. Bladder cancer: a review. *JAMA.* 2020;324:1980-1991.
3. Yang Y, Hsu PJ, Chen YS, Yang YG. Dynamic transcriptomic m(6)A decoration: writers, erasers, readers and functions in RNA metabolism. *Cell Res.* 2018;28:616-624.
4. Zaccara S, Ries RJ, Jaffrey SR. Reading, writing and erasing mRNA methylation. *Nat Rev Mol Cell Biol.* 2019;20:608-624.

5. Chen M, Wei L, Law CT, et al. RNA N6-methyladenosine methyltransferase-like 3 promotes liver cancer progression through YTHDF2-dependent posttranscriptional silencing of SOCS2. *Hepatology*. 2018;67:2254-2270.
6. Zhang S, Zhao BS, Zhou A, et al. m(6)A demethylase ALKBH5 maintains tumorigenicity of glioblastoma stem-like cells by sustaining FOXM1 expression and cell proliferation program. *Cancer Cell*. 2017;31:591-606.e6.
7. Xu C, Wang X, Liu K, et al. Structural basis for selective binding of m6A RNA by the YTHDC1 YTH domain. *Nat Chem Biol*. 2014;10:927-929.
8. Xiao W, Adhikari S, Dahal U, et al. Nuclear m(6)A reader YTHDC1 regulates mRNA splicing. *Mol Cell*. 2016;61:507-519.
9. Roundtree IA, Luo GZ, Zhang Z, et al. YTHDC1 mediates nuclear export of N(6)-methyladenosine methylated mRNAs. *eLife*. 2017;6:e31311.
10. Kasowitz SD, Ma J, Anderson SJ, et al. Nuclear m6A reader YTHDC1 regulates alternative polyadenylation and splicing during mouse oocyte development. *PLoS Genet*. 2018;14:e1007412.
11. Cheng Y, Xie W, Pickering BF, et al. N(6)-methyladenosine on mRNA facilitates a phase-separated nuclear body that suppresses myeloid leukemic differentiation. *Cancer Cell*. 2021;39:958-972.e8.
12. Liu J, Dou X, Chen C, et al. N(6)-methyladenosine of chromosome-associated regulatory RNA regulates chromatin state and transcription. *Science*. 2020;367:580-586.
13. Lesbirel S, Viphakone N, Parker M, et al. The m(6)A-methylase complex recruits TREX and regulates mRNA export. *Sci Rep*. 2018;8:13827.
14. Sheng Y, Wei J, Yu F, et al. A critical role of nuclear m6A reader YTHDC1 in leukemogenesis by regulating MCM complex-mediated DNA replication. *Blood*. 2021;138:2838-2852.
15. Liu Z, Wang T, She Y, et al. N(6)-methyladenosine-modified circIGF2BP3 inhibits CD8(+) T-cell responses to facilitate tumor immune evasion by promoting the deubiquitination of PD-L1 in non-small cell lung cancer. *Mol Cancer*. 2021;20:105.
16. Yang L, Chen Y, Liu N, et al. CircMET promotes tumor proliferation by enhancing CDKN2A mRNA decay and upregulating SMAD3. *Mol Cancer*. 2022;21:23.
17. Li F, Yi Y, Miao Y, et al. N(6)-methyladenosine modulates nonsense-mediated mRNA decay in human glioblastoma. *Cancer Res*. 2019;79:5785-5798.
18. Hou Y, Zhang Q, Pang W, et al. YTHDC1-mediated augmentation of miR-30d in repressing pancreatic tumorigenesis via attenuation of RUNX1-induced transcriptional activation of Warburg effect. *Cell Death Differ*. 2021;28:3105-3124.
19. Zhou K, Sun Y, Dong D, Zhao C, Wang W. EMP3 negatively modulates breast cancer cell DNA replication, DNA damage repair, and stem-like properties. *Cell Death Dis*. 2021;12:844.
20. Goldman MJ, Craft B, Hastie M, et al. Visualizing and interpreting cancer genomics data via the Xena platform. *Nat Biotechnol*. 2020;38:675-678.
21. Zhu ZH, Sun BY, Ma Y, et al. Three immunomarker support vector machines-based prognostic classifiers for stage IB non-small-cell lung cancer. *J Clin Oncol*. 2009;27:1091-1099.
22. Battifora H. The multitumor (sausage) tissue block: novel method for immunohistochemical antibody testing. *Lab Invest*. 1986;55:244-248.
23. Li T, Fu J, Zeng Z, et al. TIMER2.0 for analysis of tumor-infiltrating immune cells. *Nucleic Acids Res*. 2020;48:W509-W514.
24. Zhang R, Wu HX, Xu M, Xie X. KMT2A/C mutations function as a potential predictive biomarker for immunotherapy in solid tumors. *Biomark Res*. 2020;8:71.
25. Danaher P, Warren S, Dennis L, et al. Gene expression markers of tumor infiltrating leukocytes. *J Immunother Cancer*. 2017;5:18.
26. Di Timoteo G, Dattilo D, Centron-Broco A, et al. Modulation of circRNA metabolism by m(6)A modification. *Cell Rep*. 2020;31:107641.
27. Qian BZ, Pollard JW. Macrophage diversity enhances tumor progression and metastasis. *Cell*. 2010;141:39-51.
28. Conway EM, Pikor LA, Kung SH, et al. Macrophages, inflammation, and lung cancer. *Am J Respir Crit Care Med*. 2016;193:116-130.
29. Xue Y, Tong L, LiuAnwei Liu F, et al. Tumor-infiltrating M2 macrophages driven by specific genomic alterations are associated with prognosis in bladder cancer. *Oncol Rep*. 2019;42:581-594.
30. Wang Y, Yan K, Wang J, Lin J, Bi J. M2 macrophage co-expression factors correlate with immune phenotype and predict prognosis of bladder cancer. *Front Oncol*. 2021;11:609334.